A Finite Volume Trigonometric WENO Scheme for Nonlinear Degenerate Parabolic Equation*

Gulikayier Haerman, Kaiyishaer Reheman†, Muyesaier Aihemaiti, Wei Xunan
(School of Mathematics and System Sciences, Xinjiang University, Urumqi Xinjiang 830017, China)

Abstract: In this paper, we present a finite volume trigonometric weighted essentially non-oscillatory (TWENO) scheme to solve nonlinear degenerate parabolic equations that may exhibit non-smooth solutions. The present method is developed using the trigonometric scheme, which is based on zero, first, and second moments, and the direct discontinuous Galerkin (DDG) flux is used to discretize the diffusion term. Moreover, the DDG method directly applies the weak form of the parabolic equation to each computational cell, which can better capture the characteristics of the solution, especially the discontinuous solution. Meanwhile, the third-order TVD-Runge-Kutta method is applied for temporal discretization. Finally, the effectiveness and stability of the method constructed in this paper are evaluated through numerical tests.

Key words: trigonometric WENO scheme; finite volume method; nonlinear degenerate parabolic equation; TVD-Runge-Kutta method

DOI: 10.13568/j.cnki.651094.651316.2025.01.22.0002
CLC Number: O241.82 **Document Code**: A **Article ID**: 2096-7675(2026)01-0016-011
引文格式: 古丽卡依尔·哈尔曼,开依沙尔·热合曼,穆耶赛尔·艾合麦提,魏旭楠. 求解非线性退化抛物型方程的有限体积三角多项式WENO数值方法[J]. 新疆大学学报(自然科学版中英文),2026,43(1):16-26.
英文引文格式: Gulikayier Haerman, Kaiyishaer Reheman, Muyesaier Aihemaiti, Wei Xunan. A finite volume trigonometric WENO scheme for nonlinear degenerate parabolic equation[J]. Journal of Xinjiang University(Natural Science Edition in Chinese and English),2026,43(1):16-26.

求解非线性退化抛物型方程的有限体积三角多项式WENO数值方法

古丽卡依尔·哈尔曼, 开依沙尔·热合曼, 穆耶赛尔·艾合麦提, 魏旭楠
(新疆大学 数学与系统科学学院,新疆 乌鲁木齐 830017)

摘 要: 本文提出了一种有限体积框架下的三角多项式加权本质非振荡格式,以求解可能存在不光滑解的非线性退化抛物型方程. 该方法基于零阶矩、一阶矩和二阶矩重构了三角多项式WENO格式,并采用直接间断Galerkin(DDG)通量来离散扩散项. 此外,DDG方法直接将抛物型方程的弱形式应用于每个计算单元,有助于更好地捕捉解的特征,特别是间断解. 同时,采用三阶TVD-龙格-库塔法进行时间离散化. 最后通过数值测试评估所提方法的有效性和稳定性.

关键词: 三角多项式WENO格式;有限体积方法;非线性退化抛物型方程;TVD-龙格-库塔方法

* **Received Date**: 2025-01-22; **Revised Date**: 2025-09-26; **Accepted Date**: 2025-10-09.
Foundation Item: The Natural Science Foundation of Xinjiang Uygur Autonomous Region of China "RBF-Hermite difference scheme for the time-fractional kdv-Burgers equation" (2024D01C43).
Biography: Gulikayier Haerman (1994—), female, master student, research field: numerical computation of differential equations, E-mail: gulikayer@163.com.
† **Corresponding Author**: Kaiyishaer Reheman (1978—), male, associate professor, research field: numerical computation of differential equations, E-mail: kaysar106@xju.edu.cn.

0 Introduction

In this paper, we focus on designing a finite-volume TWENO scheme to solve the scalar one-dimensional (1D) nonlinear degenerate parabolic equations:

$$w_t = \Psi(w)_{xx},\ x \in [x_l, x_r],\ t > 0, \tag{1}$$

where $w = w(x, t)$ and $\Psi(w) \geqslant 0$. The equation (1) degenerates when $\Psi(w) = 0$. Parabolic equations, which are nonlinear and possibly highly degenerate, are frequently used in various fields, including Thomson model[1], plasma collisional transport models[2] and the flow of liquids and gasses in porous media[3], and others. Unfortunately, it is difficult to obtain exact solutions to such parabolic equations, so it is necessary to develop effective numerical methods to obtain approximate solutions. There have been several methods to approximate equation (1), including kinetic schemes[4], local DG (LDG) schemes[5], finite volume schemes[6], finite element schemes[7], and WENO schemes[8–13], et al. Moreover, nonlinear degenerate parabolic equations exhibit the possibility of non-smooth sharp solutions and finite propagation velocities of wave fronts, showing hyperbolic behavior. In this study, we are interested in developing a finite volume WENO scheme.

The WENO scheme has been extensively investigated for solving hyperbolic conservation laws. It exhibits good properties, including conservation, high-order accuracy in smooth areas, and non-oscillatory near discontinuities. Therefore, the WENO scheme is capable of solving equation (1). Liu et al.[14] introduced the original WENO scheme in the finite volume framework, which achieves $k + 1$ order accuracy in smooth regions. Jiang et al.[15] later proposed an arbitrary $2k - 1$ order accuracy WENO scheme within the finite difference scheme. Since then, various efficient conservative finite volume and finite difference WENO schemes have been proposed for hyperbolic conservation laws using reconstruction methods[16–20]. Recently, Liu et al.[8] firstly developed the finite difference direct WENO (DWENO) scheme for solving equation (1). Nevertheless, the mapped nonlinear weights and negative linear weights pose drawbacks for the proposed scheme in achieving high-order accuracy. Subsequently, Abedian et al.[9] employed four small stencils to form one big stencil, aiming to circumvent the issue of negative linear weights. Abedian[10] then developed a finite difference WENO scheme based on a reconstruction framework. This scheme allows for the use of any artificial positive linear weights, as long as their sum equals one. Furthermore, Abedian et al.[11] introduced a novel sixth-order WENO method specifically designed for solving degenerate parabolic equations. This method incorporates exponential polynomials to enhance its performance. Jiang[21] explored an alternative formulation for solving degenerate parabolic equations. This formulation relies on interpolations rather than reconstruction and can be readily extended to higher orders. Ahmat et al.[13] proposed a hybrid finite volume HWENO scheme. In this scheme, the DDG flux is utilized to discretize the second derivative term, and HWENO reconstruction is applied to troubled cells, while linear reconstruction is used in other regions. This innovative approach effectively reduces spurious numerical oscillations and improves the resolution of the solution.

Trigonometric polynomial reconstruction has made notable progress over the years. In 1976, Baron[22] proposed a Neville-like trigonometric interpolation algorithm. However, it was not directly applicable to the design of high-order ENO schemes. In 1996, Christofi[23] introduced a novel local trigonometric polynomial interpolation method. This approach allowed for the sequential addition of interpolation points to the stencil, facilitating the creation of high-order trigonometric ENO schemes. Building on this, Zhu et al.[24] developed a fifth-order finite difference trigonometric WENO scheme to solve hyperbolic conservation laws. Leveraging the same trigonometric polynomial basis as in [24], a new fifth-order trigonometric WENO scheme[25] was subsequently formulated for hyperbolic conservation problems. It was also applied as a limiter in Runge-Kutta DG methods. In summary, numerical methods relying on trigonometric polynomial reconstruction generally outperform those based on algebraic polynomials, especially in complex smooth regions and near strong discontinuities.

Inspired by the concept that any artificial positive linear weights (summing to one) can be applied in WENO

schemes[10,20,25-26], we note that the new TWENO schemes[25–26] are more robust and outperform traditional ones, offering distinct advantages in handling complex problems. Unlike the DG method[27], which requires rewriting the equation into a first-order system, the LDG method was discussed in [28]. However, both the DG and LDG methods depend on repeated integration by parts for the diffusion term. In contrast, the DDG flux[29], grounded in the direct weak formulation for parabolic equation solutions with only a single integration by parts, ensures consistency and conservativeness. Consequently, we propose a finite volume TWENO scheme that employs the DDG flux as the numerical flux for the diffusion term in degenerate parabolic equations.

The following is the main structure of this paper. Section 1 details the construction of the finite volume trigonometric WENO scheme. Section 2 presents numerical test results. Section 3 gives the conclusion.

1 Finite Volume Trigonometric WENO Scheme in 1D

In this section, we investigate the trigonometric WENO scheme to solve equation (1). Assume that, we have a uniform mesh on the $[x_l, x_r]$, where the target cell is $S_j = [x_{j-\frac{1}{2}}, x_{j+\frac{1}{2}}]$ with a width $h = x_{j+\frac{1}{2}} - x_{j-\frac{1}{2}}$, and cell center is $x_j = \frac{1}{2}(x_{j+\frac{1}{2}} + x_{j-\frac{1}{2}})$. Then integrating (1) over the target cell S_j and dividing by h obtain:

$$\int_{S_j} \frac{1}{h} w_t \mathrm{d}x = \int_{S_j} \frac{1}{h} \Psi(w)_{xx} \mathrm{d}x, \tag{2}$$

it is evident that

$$\frac{\mathrm{d}\bar{w}(j,t)}{\mathrm{d}t} = \frac{1}{h}\left(\Psi(w(x_{j+\frac{1}{2}},t))_x - \Psi(w(x_{j-\frac{1}{2}},t))_x\right), \tag{3}$$

where

$$\bar{w}(j,t) = \frac{1}{h}\int_{S_j} w(\sigma,t)\mathrm{d}\sigma, \tag{4}$$

is the cell average. Let $\Psi := \Psi(w, w_x) = \Psi'(w)w_x$. We approximate equation (1) by the following conservative scheme:

$$\frac{\mathrm{d}\bar{w}_j(t)}{\mathrm{d}t} = \frac{1}{h}\left(\hat{\Psi}_{j+\frac{1}{2}} - \hat{\Psi}_{j-\frac{1}{2}}\right), \tag{5}$$

we refer to $\hat{\Psi}_{j+\frac{1}{2}}$ and $\hat{\Psi}_{j-\frac{1}{2}}$ as the numerical fluxes. In this paper, we consider the DDG flux for the diffusion term. Readers can refer to reference [29] for more detailed information regarding the DDG flux with various coefficient selections. We will adopt the following notation for this flux:

$$\hat{\Psi} = D_x\Psi(w) = a_0\frac{[\Psi(w)]}{h} + \overline{\Psi(w)_x} + a_1 h[\Psi(w)_{xx}], \tag{6}$$

where $[w] = w^+ - w^-$, $\bar{w} = (w^+ + w^-)/2$ and the numerical flux $\hat{\Psi}$ at the $x_{j+\frac{1}{2}}$ is conservative. To obtain the numerical fluxes in equation (6), we need to reconstruct $w^{\pm}_{j+\frac{1}{2}}$, $(w_x)^{\pm}_{j+\frac{1}{2}}$ and $(w_{xx})^{\pm}_{j+\frac{1}{2}}$. Now, we describe the reconstruction procedures of $w^-_{j+\frac{1}{2}}$, $(w_x)^-_{j+\frac{1}{2}}$ and $(w_{xx})^-_{j+\frac{1}{2}}$.

Step 1 Choose a big stencil $\mathcal{S}_0 = \{S_{j-2}, S_{j-1}, S_j, S_{j+1}, S_{j+2}\}$ and reconstruct a quartic trigonometric polynomial $p_0(x) \in \mathrm{span}\{1, \sin(x-x_j), \cos(x-x_j) - \sin(\frac{h}{2})/\frac{h}{2}, \sin(2(x-x_j)), \cos(2(x-x_j)) - \frac{\sin(h)}{h}\}$, which satisfies

$$\frac{1}{h}\int_{x_{j+l-\frac{1}{2}}}^{x_{j+l+\frac{1}{2}}} p_0(x)\mathrm{d}x = \bar{w}_{j+l}, \qquad l = -2, -1, 0, 1, 2. \tag{7}$$

On the stencils $\mathcal{S}_1 = \{S_{j-1}, S_j\}$ and $\mathcal{S}_2 = \{S_j, S_{j+1}\}$, we reconstruct two linear trigonometric polynomials $p_1(x), p_2(x) \in \mathrm{span}\{1, \sin(x-x_j)\}$, which satisfies:

$$\begin{aligned}&\frac{1}{h}\int_{x_{j+l-\frac{1}{2}}}^{x_{j+l+\frac{1}{2}}} p_1(x)\mathrm{d}x = \bar{w}_{j+l}, && l = -1, 0,\\ &\frac{1}{h}\int_{x_{j+l-\frac{1}{2}}}^{x_{j+l+\frac{1}{2}}} p_2(x)\mathrm{d}x = \bar{w}_{j+l}, && l = 0, 1.\end{aligned} \tag{8}$$

Let $p_m(x)$ for $m = 0, 1, 2$. The derivative of $p_m(x)$ with respect to x is denoted as $\mathrm{d}p_m(x) = \partial p_m/\partial x$ when $m = 0, 1, 2$. Since it will be used later, the second derivative of $p_m(x)$ is denoted as $\mathrm{dd}p_m(x) = \partial^2 p_m/\partial x^2 (m = 0, 1, 2)$.

Step 2[30] The trigonometric polynomial $p_0(x)$ and $\mathrm{d}p_0(x)$ are rewritten as:

$$\begin{aligned}p_0(x) &= \gamma_0\left(\frac{1}{\gamma_0}p_0(x) - \frac{\gamma_0}{\gamma_1}p_1(x) - \frac{\gamma_2}{\gamma_0}p_2(x)\right) + \gamma_1 p_1(x) + \gamma_2 p_2(x),\\ \mathrm{d}p_0(x) &= \gamma_0\left(\frac{1}{\gamma_0}\mathrm{d}p_0(x) - \frac{\gamma_0}{\gamma_1}\mathrm{d}p_1(x) - \frac{\gamma_2}{\gamma_0}\mathrm{d}p_2(x)\right) + \gamma_1\mathrm{d}p_1(x) + \gamma_2\mathrm{d}p_2(x),\end{aligned} \tag{9}$$

the equation (9) is satisfied by any positive linear weights $\gamma_0, \gamma_1, \gamma_2$, provided that $\gamma_0 + \gamma_1 + \gamma_2 = 1$.

Step 3 To measure the smoothness of functions $p_m(x)$ for $m = 0, 1, 2$ within the target cell S_j, we compute the smoothness indicators β_m for $m = 0, 1, 2$. These indicators are defined in a specific manner, as detailed in reference [15]:

$$\beta_m = \sum_{l=1}^{n}\int_{S_j} h^{2l-1}\left(\frac{\mathrm{d}^l p_m(x)}{\mathrm{d}x^l}\right)^2 \mathrm{d}x, \tag{10}$$

where $m = 0, 1, 2$, $n = 4$ for $m = 0$ while $n = 1$ for $m = 1, 2$.

Step 4 To introduce nonlinear weights ω_0, ω_1 and ω_2, we first measure the absolute difference of smoothness indicators as $\tau = ((|\beta_0 - \beta_1| + |\beta_0 - \beta_2|)/2)^2$ and the nonlinear weights ω_m are defined as:

$$\omega_m = \frac{\bar{\omega}_m}{\sum_{l=0}^{2}\bar{\omega}_l}, \quad \bar{\omega}_m = \gamma_m + \left(\frac{\tau}{\varepsilon + \beta_m}\right), \quad m = 0, 1, 2, \tag{11}$$

where ε represents a small positive number, which is introduced to prevent the denominator from becoming 0. In this paper, for the purpose of our computation, we simply set $\varepsilon = 10^{-8}$.

Step 5 We replace the linear weights in (9) with nonlinear weights (11), obtain the approximation of $w(x^-_{j+\frac{1}{2}}, t)$, $w_x(x^-_{j+\frac{1}{2}}, t)$ and $w_{xx}(x^-_{j+\frac{1}{2}}, t)$:

$$\begin{aligned}w^-_{i+\frac{1}{2}} &= \omega_0\left(\frac{1}{\gamma_0}p_0(x_{j+\frac{1}{2}}) - \frac{\gamma_1}{\gamma_0}p_1(x_{j+\frac{1}{2}}) - \frac{\gamma_2}{\gamma_0}p_2(x_{j+\frac{1}{2}})\right) + \omega_1 p_1(x_{j+\frac{1}{2}}) + \omega_2 p_2(x_{j+\frac{1}{2}}),\\ (w_x)^-_{i+\frac{1}{2}} &= \omega_0\left(\frac{1}{\gamma_0}\mathrm{d}p_0(x_{j+\frac{1}{2}}) - \frac{\gamma_1}{\gamma_0}\mathrm{d}p_1(x_{j+\frac{1}{2}}) - \frac{\gamma_2}{\gamma_0}\mathrm{d}p_2(x_{j+\frac{1}{2}})\right) + \omega_1\mathrm{d}p_1(x_{j+\frac{1}{2}}) + \omega_2\mathrm{d}p_2(x_{j+\frac{1}{2}}),\\ (w_{xx})^-_{i+\frac{1}{2}} &= \mathrm{dd}p_0(x_{j+\frac{1}{2}}).\end{aligned} \tag{12}$$

Finally, after completing the spatial reconstruction, for time discretization we will use the third-order total variation diminishing Runge-Kutta (TVD-RK3) method[31]:

$$\begin{cases}w^{(1)} = w^n + \Delta t L(w^n),\\ w^{(2)} = \frac{3}{4}w^n + \frac{1}{4}w^{(1)} + \frac{1}{4}\Delta t L(w^{(1)}),\\ w^{n+1} = \frac{1}{3}w^n + \frac{2}{3}w^{(2)} + \frac{2}{3}\Delta t L(w^{(2)}).\end{cases} \tag{13}$$

2 Numerical Tests

In this section, we present the numerical results of the finite volume TWENO scheme described in the previous sections for one dimensional nonlinear degenerate parabolic equations. For stability, we choose the time step for 1D problems:

$$u_t + f(w)_x = \Psi(w)_{xx}, \tag{14}$$

as $\Delta t = CFL/\left(\frac{\max\left|f'(w)\right|}{h} + \frac{\max\left|\Psi'(w)\right|}{h^2}\right)$ with $CFL = 0.3$, and we use the Lax-Friedrichs flux for the convection term. Furthermore, we take into account numerical methods for comparison: the current TWENO scheme, the DWENO scheme[8], and the MRWENO scheme[21].

In the following accuracy tests, we give the L^∞, L^1 and L^2 norm errors as follows:

$$\begin{aligned} L^\infty \text{error} &= \max\left(|w_j^n - w_j^{\text{exact}}|\right), \\ L^1 \text{error} &= \frac{\sum\left(|w_j^n - w_j^{\text{exact}}|\right)}{N+1}, \\ L^2 \text{error} &= \sqrt{\frac{\sum\left(|w_j^n - w_j^{\text{exact}}|^2\right)}{N+1}}, \end{aligned} \tag{15}$$

and the convergence order is defined as:

$$\text{order} = \log_2\left(\frac{E_N}{E_{2N}}\right). \tag{16}$$

Example 1 We consider the linear diffusion problem in the following form:

$$w_t = w_{xx}, \qquad x \in [-\pi, \pi]. \tag{17}$$

The initial condition for this problem is given by $w(x, 0) = \sin(x)$ and the boundary condition is periodic. The analytical solution is $w(x, t) = e^{-t}\sin(x)$. The numerical errors and convergence orders at time $t = 2$ are presented in Table 1.

Table 1 The L^∞, L^1, and L^2 norm errors and convergence orders for Example 1

N	L^∞ error	order	L^1 error	order	L^2 error	order
10	1.01×10^{-4}	-	6.52×10^{-5}	-	7.41×10^{-5}	-
20	1.59×10^{-6}	5.98	1.02×10^{-6}	5.99	1.13×10^{-6}	6.03
40	2.49×10^{-8}	5.99	1.58×10^{-8}	6.00	1.76×10^{-8}	6.00
80	2.18×10^{-9}	6.00	1.39×10^{-9}	6.00	1.54×10^{-9}	6.00

Example 2 We simulate the 1D PME ($m > 1$):

$$w_t = \left(w^m\right)_{xx}, \tag{18}$$

the Barenblatt solution of (18) is given as:

$$B_m(x,t) = t^{-k}\left[\left(1 - \frac{k(m-1)}{2m}\frac{|x|^2}{t^{2k}}\right)_+\right]^{\frac{1}{m-1}}, \quad m > 1, \tag{19}$$

with $k = 1/(m+1)$ and $w_+ = \max(w, 0)$. The initial condition of this problem is obtained by deriving from the Barenblatt solution when $t = 1$, and the boundary condition is $w(\pm6, t) = 0$.

In Figure 1, we plot the results of PME for different values of m using the DWENO, MRWENO and TWENO schemes with $N = 200$. We can clearly see that the TWENO method behaves much better compared to the other methods at the degradation points.

We focus on simulating the collision of two initial boxes with the same heights when $m = 5$ in equation (18). The initial condition is given by:

$$w(x,0) = \begin{cases} 1, & x \in (-3.7, -0.7) \cup (0.7, 3.7), \\ 0, & \text{otherwise}. \end{cases} \tag{20}$$

In Figure 2, we show the results at different time levels for the three schemes with $N = 180$. Additionally, Figure 3 compares the results at $t = 0.3$ for the DWENO, MRWENO, and TWENO schemes with $N = 180$. We can clearly see that the TWENO scheme performs well. In all our computations, the reference solution is computed using the HWENO scheme[12] with $N = 2\,000$ grid points.

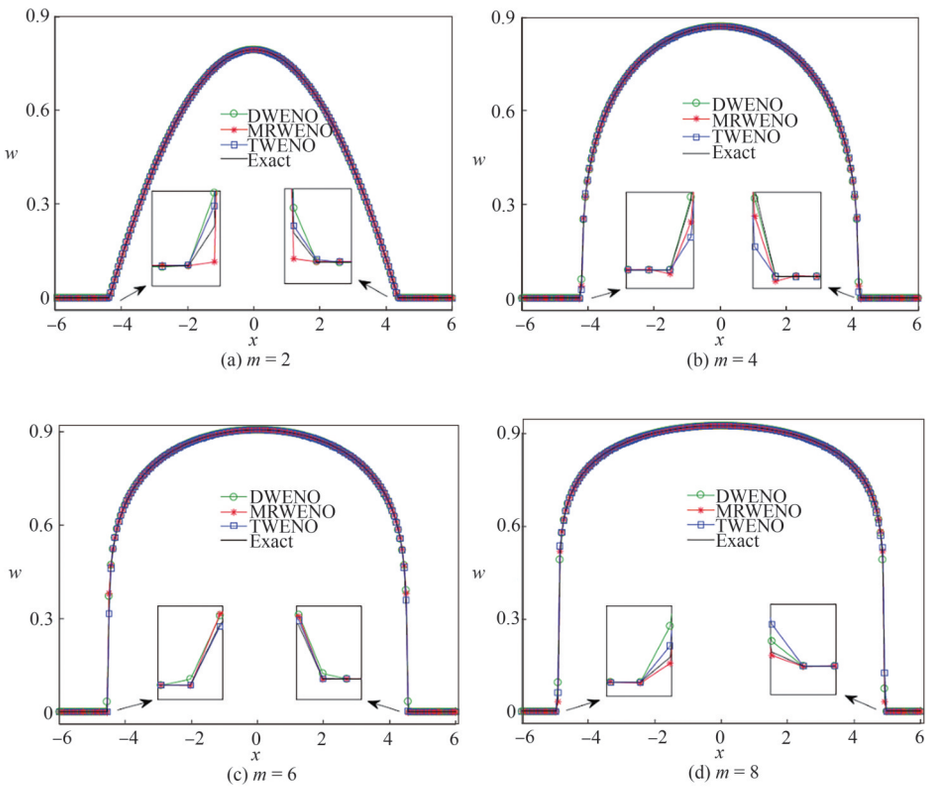

Figure 1 Barenblatt solution for PME in Example 2

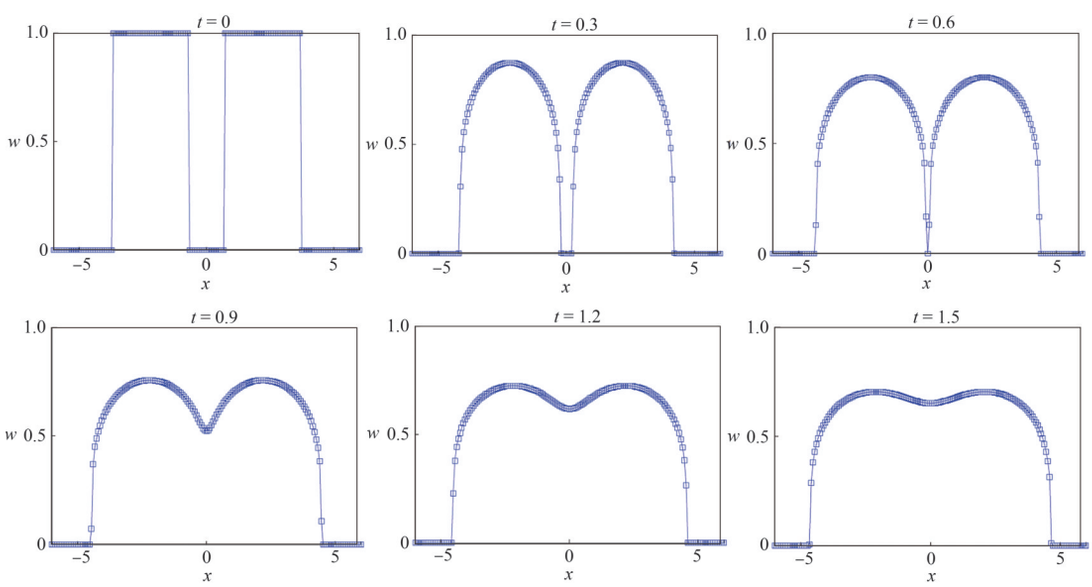

Figure 2 The two-box problem with the same heights at different time

Next, we consider the collision of two initial boxes with different heights when $m = 6$ in equation (18). The initial condition is as follows:

$$w(x,0) = \begin{cases} 1, & x \in (-4,-1), \\ 2, & x \in (0,3), \\ 0, & \text{otherwise}. \end{cases} \tag{21}$$

In Figure 4, we show the results at different time levels for the three schemes with $N = 180$. Moreover, Figure 5 compares the results at $t = 0.12$ for the DWENO, MRWENO, and TWENO schemes with $N = 180$. We can clearly see that the TWENO scheme performs well, while the results of the DWENO and MRWENO schemes are oscillatory.

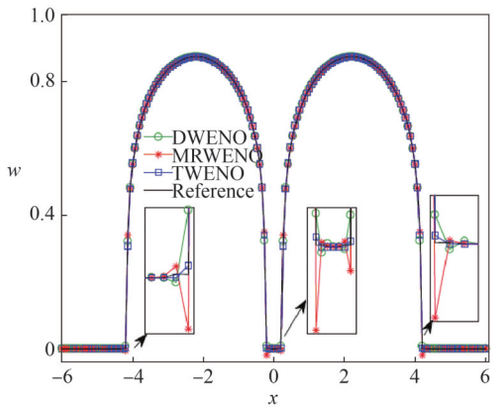

Figure 3 The two-box problem with the same height at $t = 0.3$ in Example 2

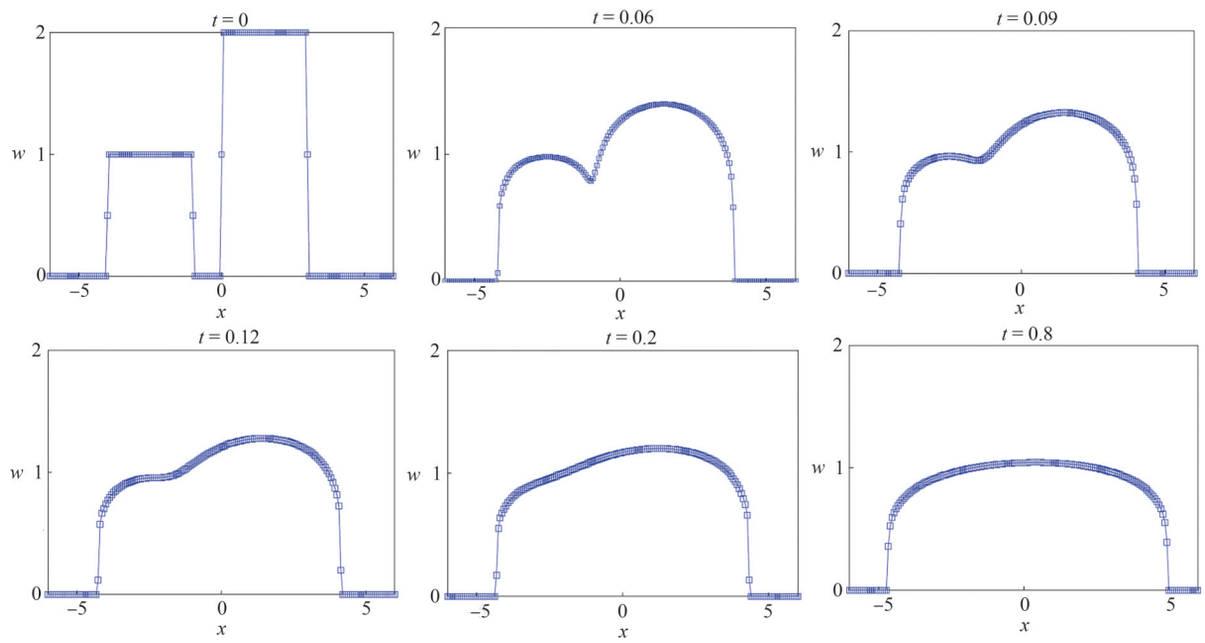

Figure 4 The two-box problem with the different heights at different times

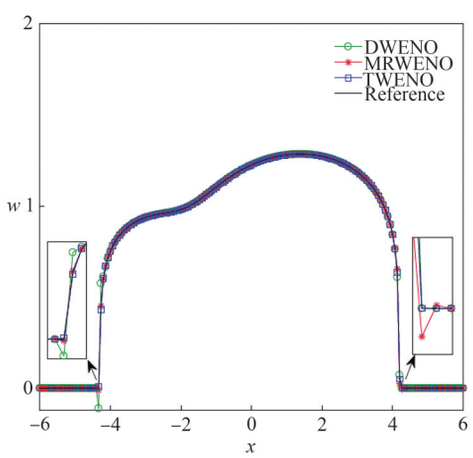

Figure 5 The two-box problem with the different heights at $t = 0.12$ in Example 2

Example 3 Now, we consider the nonlinear Buckley-Leverett equation, which can be used to model two-phase flow in oil reservoirs. The equation is given by:

$$w_t + f(w)_x = \varepsilon\left(v(w)w_x\right)_x, \quad \varepsilon v(w) \geqslant 0, \tag{22}$$

we define the functions as follows:

$$f(w)=\frac{w^2}{w^2+(1-w)^2},\quad v(w)=4w(1-w), \tag{23}$$

and we set $\varepsilon=0.01$. In this example, we will simulate the solution to this problem with the fluxes (23) and the following initial condition:

$$w(x,0)=\begin{cases}1-3x, & 0\leqslant x\leqslant\dfrac{1}{3},\\ 0, & \dfrac{1}{3}<x\leqslant 1,\end{cases} \tag{24}$$

with the inflow and outflow boundary conditions. Figure 6 compares the results at $t=0.2$ and $t=0.5$ for DWENO, MRWENO, and TWENO schemes with $N=200$, indicating that the numerical result of the TWENO method can converge to the entropy solution.

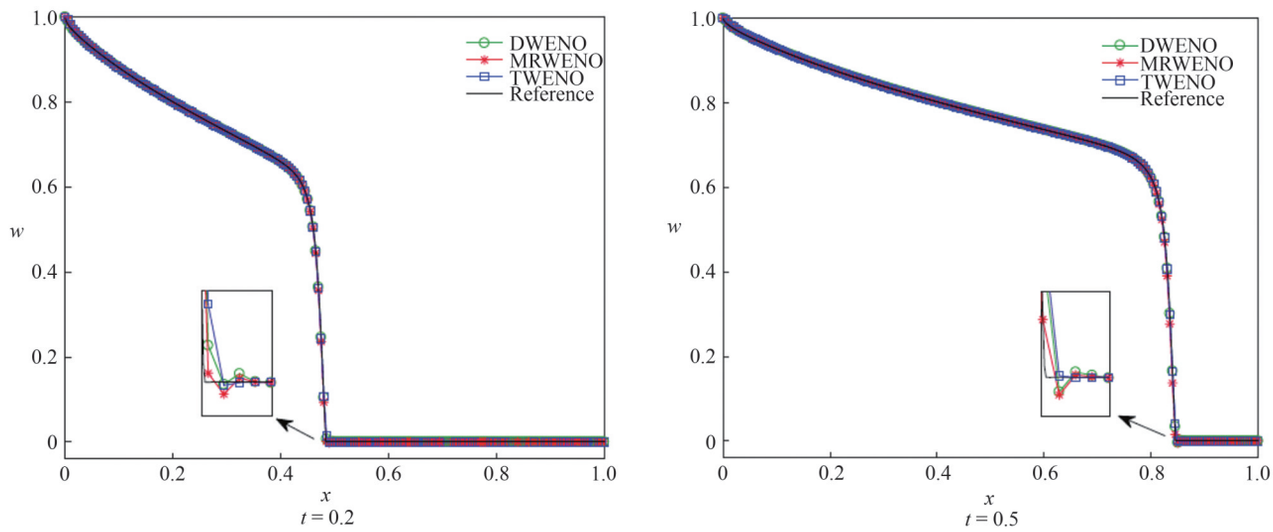

Figure 6 The numerical solution of the Buckley-Leverett in Example 3

Following this, to test the non-gravitational effects on the Buckley-Leverett equation, we consider the fluxes (23) and initial data as follows:

$$w(x,0)=\begin{cases}0, & 0\leqslant x<1-\dfrac{1}{\sqrt{2}},\\ 1, & 1-\dfrac{1}{\sqrt{2}}\leqslant x\leqslant 1,\end{cases} \tag{25}$$

with $w(0,t)=0$ and $w(1,t)=1$. We present the results of the DWENO, MRWENO, and TWENO schemes with $N=200$ at $t=0.2$, 0.5 in Figure 7. Notice that our method can accurately solve it without oscillations, which is more than the other two schemes.

Finally, we test the gravitational effects on the Buckley-Leverett equation with the same initial data in (25), and with the gravitational function given as:

$$f(w)=\frac{w^2}{w^2+(1-w)^2}\left(1-5(1-w)^2\right). \tag{26}$$

Figure 8 displays the results of the DWENO, MRWENO, and TWENO schemes with $N=200$ at $t=0.1$, 0.2. We notice that the TWENO scheme approaches the entropy solution near the degenerate point without oscillations, while the other two schemes exhibit smaller fluctuations.

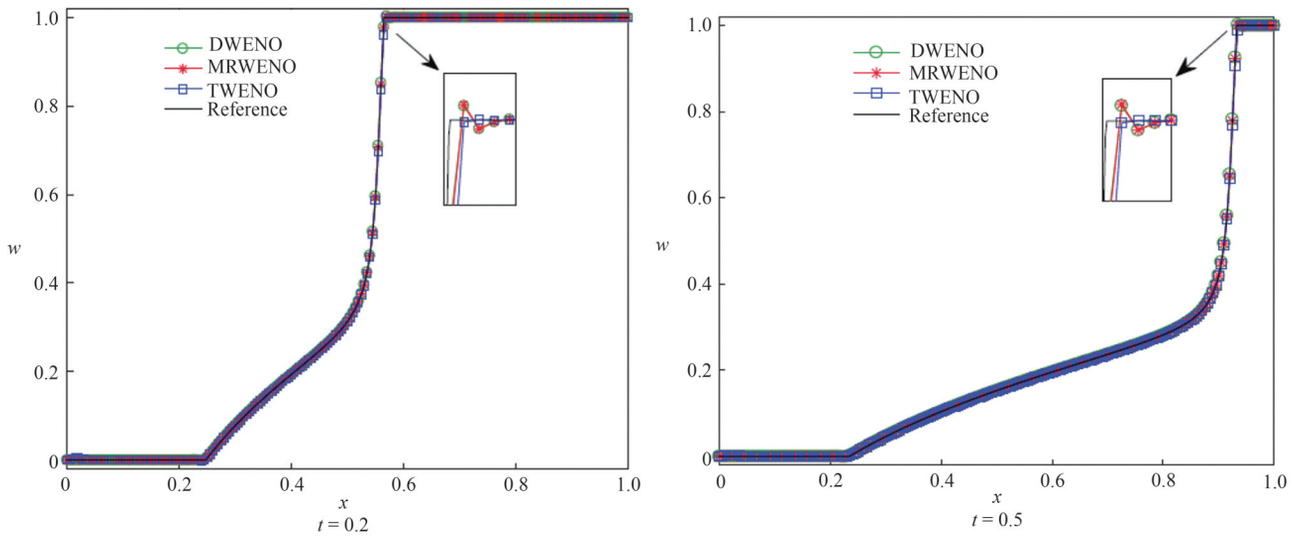

Figure 7 The Riemann problem of the Buckley-Leverett equation at $t = 0.2, 0.5$ in Example 3

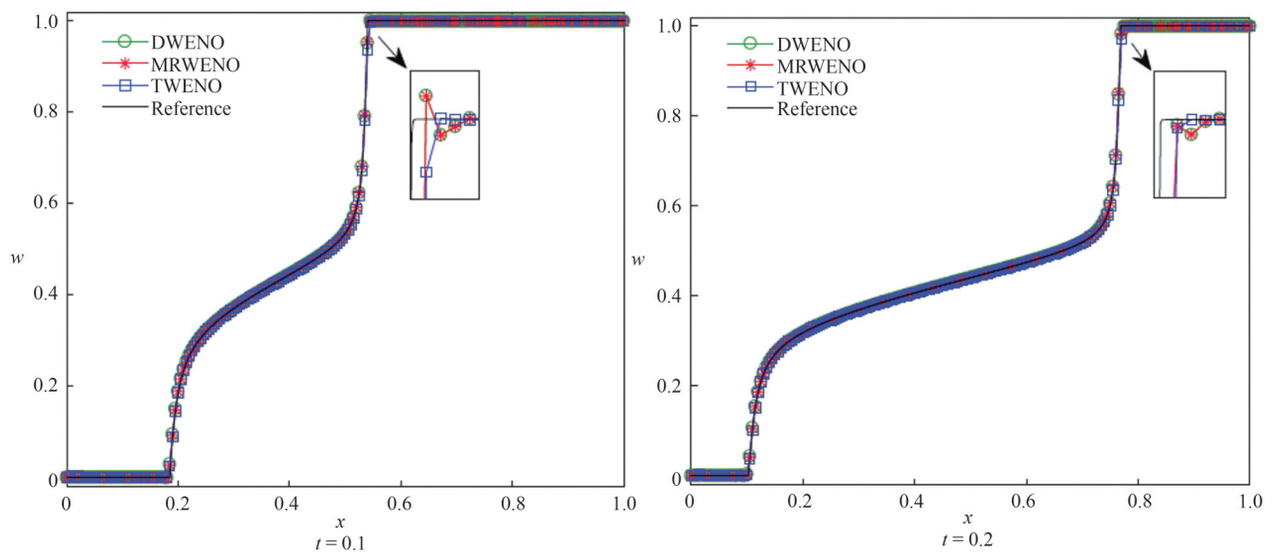

Figure 8 The Riemann problem of the Buckley-Leverett equation at $t = 0.1, 0.2$ in Example 3

Example 4 As the final example, we solve a strongly degenerate parabolic equation in the form of (22) with $\varepsilon = 0.1$ and the following fluxes:

$$f(w) = w^2,\ v(w) = \begin{cases} 0, & |w| \leqslant 0.25, \\ 1, & |w| > 0.25. \end{cases} \tag{27}$$

For this problem, we consider the following initial condition:

$$w(x,0) = \begin{cases} 1, & -\dfrac{1}{\sqrt{2}} - 0.4 < x < -\dfrac{1}{\sqrt{2}} + 0.4, \\ -1, & \dfrac{1}{\sqrt{2}} - 0.4 < x < \dfrac{1}{\sqrt{2}} + 0.4, \\ 0, & \text{otherwise}, \end{cases} \tag{28}$$

the boundary condition is taken as $w(\pm 2,\ t) = 0$. Figure 9 depicts the numerical solutions for DWENO, MRWENO, and TWENO schemes at $t = 0.4$ and $t = 0.8$ with $N = 280$. In this test case, the TWENO scheme produces better results with a higher resolution.

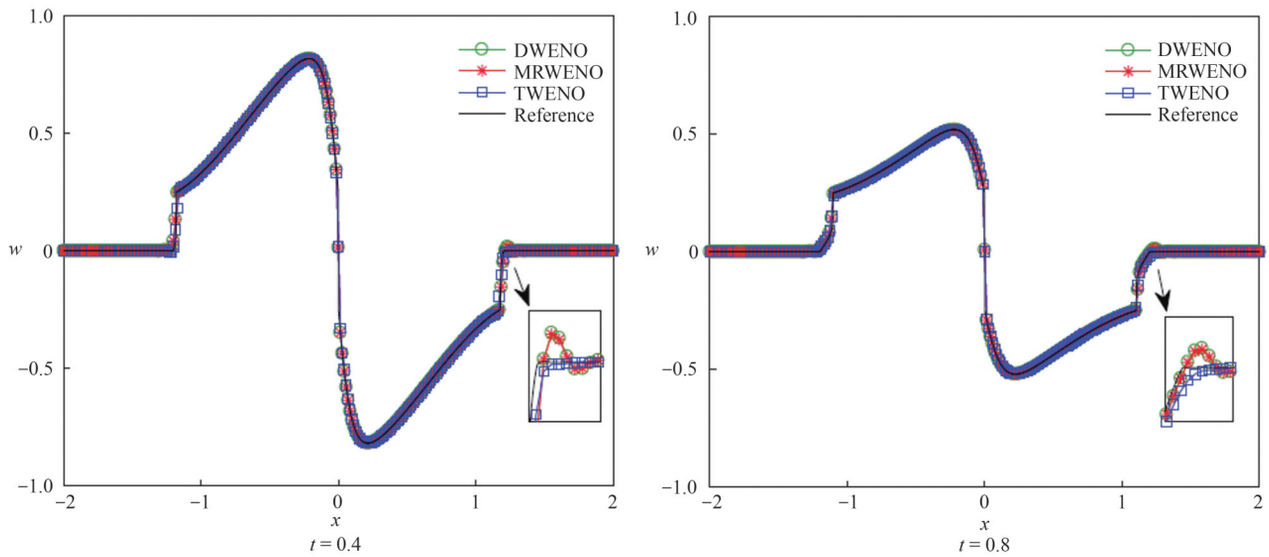

Figure 9 The numerical solution of Example 4 at $t = 0.4, 0.8$

3 Conclusion

In conclusion, the finite volume trigonometric weighted essentially non-oscillatory scheme proposed in this paper is effective for solving nonlinear degenerate parabolic equations with non-smooth solutions. Initially, we combine the TWENO scheme and the DDG flux for the diffusion term, which can accurately capture the solution characteristics, especially discontinuities. Subsequently, the third-order TVD-Runge-Kutta method ensures stable and accurate temporal discretization. Finally, numerical tests show the effectiveness and stability of our method. In the future, we may extend this approach to more complex equations or multi-dimensional problems.

References:

[1] Pikulin S V. The Thomas-Fermi problem and solutions of the Emden-Fowler equation[J]. Computational Mathematics and Mathematical Physics, 2019, 59(8): 1292-1313.

[2] Ghosh D, Dorf M A, Dorr M R, et al. Kinetic simulation of collisional magnetized plasmas with semi-implicit time integration[J]. Journal of Scientific Computing, 2018, 77(2): 819-849.

[3] Aronson D G. The porous medium equation[C]//Nonlinear Diffusion Problems: Lectures given at the 2nd 1985 Session of the Centro Internazionale Matermatico Estivo (CIME) held at Montecatini Terme, June 10-18, 1985, Berlin, Heidelberg: Springer Berlin Heidelberg, 2006: 1-46.

[4] Aregba-Driollet D, Natalini R, Tang S. Explicit diffusive kinetic schemes for nonlinear degenerate parabolic systems[J]. Mathematics of Computation, 2004, 73(245): 63-94.

[5] Zhang Q, Wu Z L. Numerical simulation for porous medium equation by local discontinuous Galerkin finite element method[J]. Journal of Scientific Computing, 2009, 38(2): 127-148.

[6] Bessemoulin-Chatard M, Filbet F. A finite volume scheme for nonlinear degenerate parabolic equations[J]. SIAM Journal on Scientific Computing, 2012, 34(5): B559-B583.

[7] Radu F A, Pop I S, Knabner P. Newton: Type methods for the mixed finite element discretization of some degenerate parabolic equations[C]//Numerical Mathematics and Advanced Applications: Proceedings of ENUMATH 2005, the 6th European Conference on Numerical Mathematics and Advanced Applications Santiago de Compostela, July 2005, Berlin, Heidelberg: Springer Berlin Heidelberg, 2006: 1192-1200.

[8] Liu Y Y, Shu C W, Zhang M P. High order finite difference WENO schemes for nonlinear degenerate parabolic equations[J]. SIAM Journal on Scientific Computing, 2011, 33(2): 939-965.

[9] Abedian R, Adibi H, Dehghan M. A high-order weighted essentially non-oscillatory (WENO) finite difference scheme for nonlinear degenerate parabolic equations[J]. Computer Physics Communications, 2013, 184(8): 1874-1888.

[10] Abedian R. A new high-order weighted essentially non-oscillatory scheme for non-linear degenerate parabolic equations[J]. Numerical Methods for Partial Differential Equations,2021,37(2):1317-1343.

[11] Abedian R,Dehghan M. A high-order weighted essentially nonoscillatory scheme based on exponential polynomials for nonlinear degenerate parabolic equations[J]. Numerical Methods for Partial Differential Equations,2022,38(4):970-996.

[12] Ahmat M,Ni S Y,Zhang M,et al. A sixth-order finite difference HWENO scheme for nonlinear degenerate parabolic equation[J]. Computers & Mathematics with Applications,2023,150:196-210.

[13] Ahmat M,Qiu J X. Hybrid HWENO method for nonlinear degenerate parabolic equations[J]. Journal of Scientific Computing,2023,96(3):83.

[14] Liu X D,Osher S,Chan T. Weighted essentially non-oscillatory schemes[J]. Journal of Computational Physics,1994,115(1):200-212.

[15] Jiang G S,Shu C W. Efficient implementation of weighted ENO schemes[J]. Journal of Computational Physics,1996,126(1):202-228.

[16] Borges R,Carmona M,Costa B,et al. An improved weighted essentially non-oscillatory scheme for hyperbolic conservation laws[J]. Journal of Computational Physics,2008,227(6):3191-3211.

[17] Castro M,Costa B,Don W S. High order weighted essentially non-oscillatory WENO-Z schemes for hyperbolic conservation laws[J]. Journal of Computational Physics,2011,230(5):1766-1792.

[18] Levy D,Puppo G,Russo G. Compact central WENO schemes for multidimensional conservation laws[J]. SIAM Journal on Scientific Computing,2000,22(2):656-672.

[19] Zhu J,Qiu J X. A new fifth order finite difference WENO scheme for solving hyperbolic conservation laws[J]. Journal of Computational Physics,2016,318:110-121.

[20] Zhu J,Qiu J X. A new type of finite volume WENO schemes for hyperbolic conservation laws[J]. Journal of Scientific Computing,2017,73(2):1338-1359.

[21] Jiang Y. High order finite difference multi-resolution WENO method for nonlinear degenerate parabolic equations[J]. Journal of Scientific Computing,2021,86(1):1-20.

[22] Baron W. Zur trigonometrischen interpolation[J]. Computing,1976,16(4):319-328.

[23] Christofi S N. The study of building blocks for essentially non-oscillatory (ENO) schemes[M]. Providence:Brown University,1996.

[24] Zhu J,Qiu J X. Trigonometric WENO schemes for hyperbolic conservation laws and highly oscillatory problems[J]. Communications in Computational Physics,2010,8(5):1242-1263.

[25] Wang Y M,Zhu J,Xiong L L. A new fifth-order trigonometric WENO scheme for hyperbolic conservation laws and highly oscillatory problems[J]. Advances in Applied Mathematics and Mechanics,2019,11(5):1114-1135.

[26] Wang Y M,Zhu J. A new type of increasingly high-order multi-resolution trigonometric WENO schemes for hyperbolic conservation laws and highly oscillatory problems[J]. Computers & Fluids,2020,200:104448.

[27] Cheng Y D,Shu C W. A discontinuous Galerkin finite element method for time dependent partial differential equations with higher order derivatives[J]. Mathematics of Computation,2008,77(262):699-731.

[28] Xu Y,Shu C W. Local discontinuous Galerkin methods for nonlinear Schrödinger equations[J]. Journal of Computational Physics,2005,205(1):72-97.

[29] Liu H L,Yan J. The direct discontinuous Galerkin(DDG)methods for diffusion problems[J]. SIAM Journal on Numerical Analysis,2009,47(1):675-698.

[30] Jiang G S,Shu C W. Efficient implementation of weighted ENO schemes[J]. Journal of Computational Physics,1996,126(1):202-228.

[31] Shu C W,Osher S. Efficient implementation of essentially non-oscillatory shock-capturing schemes[J]. Journal of Computational Physics,1988,77(2):439-471.

责任编辑：刘 敏